Loss of insulin-induced activation of TRPM6 magnesium channels results in impaired glucose tolerance during pregnancy

Anil V. Nair[a,1], Berthold Hocher[b,c,d,1], Sjoerd Verkaart[a], Femke van Zeeland[a], Thiemo Pfab[c,e], Torsten Slowinski[c,f], You-Peng Chen[c,g], Karl Peter Schlingmann[h], André Schaller[i], Sabina Gallati[i], René J. Bindels[a], Martin Konrad[h], and Joost G. Hoenderop[a,2]

[a]Department of Physiology, Nijmegen Centre for Molecular Life Sciences, Radboud University Nijmegen Medical Centre, 6500 HB, Nijmegen, The Netherlands; [b]Institute of Nutritional Science, University of Potsdam, D-14469 Potsdam, Germany; [c]Center for Cardiovascular Research/ Institute of Pharmacology, Campus Mitte, Charité, 10115 Berlin, Germany; [d]Research and Early Development, F. Hoffmann-La Roche, BS-4070 Basel, Switzerland; [e]Department of Nephrology, Campus Benjamin Franklin, Charité, 12203, Berlin, Germany; [f]Department of Nephrology, Campus Mitte, Charité, 10117 Berlin, Germany; [g]Department of Infectious Diseases, The First Affiliated Hospital of Jinan University, Guangzhou, China; [h]Department of General Pediatrics, University Children's Hospital Münster, 48149 Münster, Germany; and [i]Division of Human Genetics, University Hospital, CH-3010 Bern, Switzerland

Edited by Makoto Tominaga, Okazaki Institute for Integrative Bioscience, Okazaki, Japan, and accepted by the Editorial Board May 31, 2012 (received for review August 23, 2011)

Hypomagnesemia affects insulin resistance and is a risk factor for diabetes mellitus type 2 (DM2) and gestational diabetes mellitus (GDM). Two single nucleotide polymorphisms (SNPs) in the epithelial magnesium channel TRPM6 ($V^{1393}I$, $K^{1584}E$) were predicted to confer susceptibility for DM2. Here, we show using patch clamp analysis and total internal reflection fluorescence microscopy, that insulin stimulates TRPM6 activity via a phosphoinositide 3-kinase and Rac1-mediated elevation of cell surface expression of TRPM6. Interestingly, insulin failed to activate the genetic variants TRPM6 ($V^{1393}I$) and TRPM6($K^{1584}E$), which is likely due to the inability of the insulin signaling pathway to phosphorylate TRPM6(T^{1391}) and TRPM6(S^{1583}). Moreover, by measuring total glycosylated hemoglobin (TGH) in 997 pregnant women as a measure of glucose control, we demonstrate that TRPM6($V^{1393}I$) and TRPM6($K^{1584}E$) are associated with higher TGH and confer a higher likelihood of developing GDM. The impaired response of TRPM6($V^{1393}I$) and TRPM6($K^{1584}E$) to insulin represents a unique molecular pathway leading to GDM where the defect is located in TRPM6.

kidney | distal convoluted tubule | transient receptor potential | vesicular trafficking

Gestational diabetes mellitus (GDM) is a condition in which women without previously diagnosed diabetes exhibit high blood glucose levels during pregnancy. Babies born to mothers with GDM are typically at increased risk of large for gestational age (LGA), low blood sugar, and jaundice (1). Women with GDM are at a higher risk for preeclampsia and Caesarean section (1) as well as developing diabetes mellitus type 2 (DM2) later in life (2). GDM affects 3–10% of pregnancies, depending on the population studied. No specific cause has been identified, but it is believed that in particular sex hormones (i.e., estrogen, progesterone, prolactin) produced during pregnancy increases a woman's resistance to insulin, resulting in impaired glucose tolerance (1, 3). Moreover, pregnant women are prone to lose magnesium (Mg^{2+}). Bardicef et al. (4) demonstrated that pregnancy itself is a condition of intracellular Mg^{2+} depletion. This depletion was more pronounced in women affected by GDM. The elevation in female hormones as well as Mg^{2+} deficiency during pregnancy impairs insulin sensitivity and these disturbances may even act synergistically.

There is growing evidence suggesting that Mg^{2+} deficiency is a significant risk factor for the development of insulin resistance and subsequently hypertension and DM2 (5–8), but the underlying molecular mechanism is unknown. The first evidence suggesting a direct connection between Mg^{2+} deficiency and the occurrence of metabolic diseases came from the identification of a monogenic disease primarily characterized by significant hypomagnesemia that was caused by a mutation in a mitochondrial tRNA (9). Moreover, in a recent genome-wide association (GWA) study, it was demonstrated that certain SNPs nominally associated with hypomagnesemia also correlate with fasting glucose levels, again supporting the hypothesis of a direct link between Mg^{2+} and metabolic defects (10). Recently, Song et al. (11) suggested by conducting a nested case control study that two common nonsynonymous SNPs of the epithelial Mg^{2+} channel TRPM6, $V^{1391}I$ and $K^{1584}E$, might confer susceptibility to DM2 in postmenopausal women with low Mg^{2+} intake.

Mg^{2+} regulates ion channels, cellular processes, and serves as a cofactor for ample essential metabolic reactions. It is involved in multiple steps of the insulin signal transduction pathways such as insulin secretion, binding, and receptor activity (5, 6, 12), suggesting that reduced intracellular Mg^{2+} decreases insulin receptor (IR) activity, impairs postreceptor action, and results in an increased insulin resistance. We thus hypothesize that pregnant women who have an altered Mg^{2+} handling are particularly prone to severe impairment of glucose tolerance or GDM. From the existing evidence, TRPM6 is considered a likely candidate molecule and the effect of insulin on TRPM6 channel activity was, therefore, studied. Using a multidisciplinary approach consisting of electrophysiological, biochemical, and live cell imaging techniques, we demonstrate that insulin stimulates TRPM6 activity, specifically through IRs, by a signaling cascade ultimately increasing the cell membrane abundance of the channel. Interestingly, the two TRPM6 SNPs, $V^{1391}I$ and $K^{1584}E$, were not activated by insulin. The clinical significance of our hypothesis was further substantiated by analyzing these specific SNPs in pregnant women from the Berlin Birth Cohort (BBC) (13, 14).

Results

Insulin Stimulates TRPM6 Channel Activity Specifically by Engaging IR. TRPM6 is expressed along the distal convoluted tubule (DCT) in the apical membrane where it reabsorbs Mg^{2+} (15) and thus plays

Author contributions: A.V.N., S.V., K.P.S., S.G., R.J.B., M.K., and J.G.H. designed research; A.V.N., S.V., F.v.Z., and Y.-P.C. performed research; A.V.N., S.V., T.P., T.S., A.S., R.J.B., and J.G.H. analyzed data; B.H. designed and analyzed clinical study; T.P. and T.S. collected and analyzed clinical data; Y.-P.C. collected clinical data and took total glycolsylated hemoglobin measurements; K.P.S. designed the clinical study; A.S. performed clinical data analysis and genotyping; S.G. designed the association study; M.K. designed the clinical study; and A.V.N., B.H., S.V., R.J.B., M.K., and J.G.H. wrote the paper.

The authors declare no conflict of interest.

This article is a PNAS Direct Submission. M.T. is a guest editor invited by the Editorial Board.

[1]A.V.N. and B.H. contributed equally to this work.

[2]To whom correspondence should be addressed. E-mail: J.Hoenderop@fysiol.umcn.nl.

This article contains supporting information online at www.pnas.org/lookup/suppl/doi:10.1073/pnas.1113811109/-/DCSupplemental.

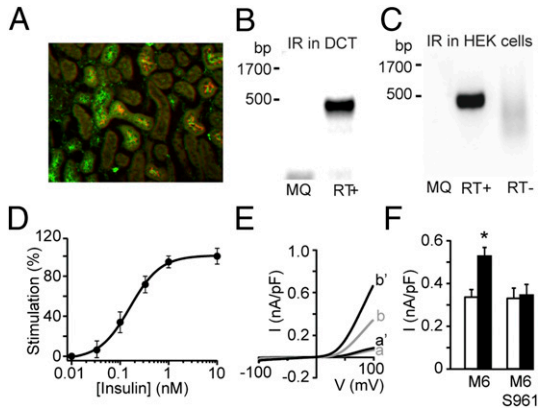

Fig. 1. Insulin activates TRPM6 channels by specifically engaging IR. (*A*) Immunohistochemical costaining of the insulin receptor (IR, in green) and the Na^+,Cl^- cotransporter (NCC, in red) on renal mouse sections. (*B*) mRNA transcripts of IR were identified in the COPAS sorted DCT fragments using PCR. (*C*) Similarly, the IR expression in HEK293T cells was identified. Milli-Q water was taken as a control. (*D*) Dose–response curve of insulin-induced current in TRPM6-transfected HEK293T cells indicating half maximal effective concentration of 0.16 nM (n = 17–43). (*E*) The I/V relationship of cells transfected with plasmids of mock (*a*, n = 9), mock pretreated with 10 nM of insulin (*a′*, n = 10), TRPM6 (*b*, n = 43), and TRPM6 pretreated with 10 nM of insulin (*b′*, n = 24). (*F*) Averaged current density (nA/pF) at +80 mV of TRPM6-transfected HEK293T cells, pretreated with 10 nM S961, the IR blocker, with (■) or without (□) insulin pretreatment.

a pivotal role in Mg^{2+} homeostasis. To study the expression of the IR in this Mg^{2+}-transporting segment, we performed immunohistochemistry on mouse kidney sections, indicating costaining of IR and Na^+,Cl^-cotransporter (NCC), a known marker of DCT (Fig. 1*A*). Furthermore, complex object parametric analyzer and sorter (COPAS) large particle flow cytometry was applied to collect the DCT segments of mouse kidney. The expression of IR in this segment was confirmed by PCR analysis and a single band of the expected molecular size (Fig. 1*B*) was detected. The purity of the DCT preparation was evaluated by PCR expression profiling using specific nephron makers and negative controls (Fig. S1*A*). Quantitative PCR analysis indicated highly enriched expression of the known DCT markers parvalbumin (19-fold), TRPM6 (17-fold), and NCC (25-fold) compared with total renal expression. In contrast, expression of the Na^+,K^+,$2Cl^-$ cotransporter (NKCC2) and aquaporin 2 (AQP2) is low underlining the DCT origin of the tubular preparation (Fig. S1*A*).

Human embryonic kidney 293T (HEK293T) cells, which express the IR (Fig. 1*C*), were used to investigate the effect of insulin on TRPM6 activity. HEK293T cells were transiently transfected with TRPM6 and subsequently analyzed by the whole-cell patch clamp method. Insulin stimulated TRPM6 activity and reached a maximal activation at 1 h of treatment (Fig. S1*B*). Insulin stimulated TRPM6 activity in a dose-dependent manner with an EC_{50} of 0.16 nM and with a maximally increased current at 10 nM (Fig. 1*D*). The characteristic outwardly rectifying current–voltage (I/V) relationship of TRPM6 was not affected by the insulin application (Fig. 1*E*). The current recorded from mock-transfected cells was also unaltered by insulin treatment (Fig. 1*E*). To address whether the stimulatory action of insulin was specifically mediated by IR, TRPM6-expressing HEK293T cells were incubated with 10 nM of S961, a specific IR antagonist (16). A subsaturating concentration of insulin (0.9 nM) was applied to minimize ligand competition between insulin and the antagonist. Insulin (0.9 nM) was added 20 min after applying S961 to the bath solution and now the stimulatory action of insulin was not observed (Fig. 1*F*). Moreover, 10 nM of S961 alone had no effect on basal TRPM6 activity including the I/V relationship (Fig. 1*F* and Fig. S1*C*).

TRPM6 Residues V^{1393} and K^{1584} Are Essential for the Stimulatory Action of Insulin. Contrary to wild-type TRPM6, insulin did not stimulate the channels harboring $V^{1393}I$ and $K^{1584}E$ (Fig. 2*A*). The I/V relations of the two SNPs were similar to that of the wild-type TRPM6 (Fig. 2*B*). Importantly, Western blots analysis of total cell lysates expressing the TRPM6 variants indicated that they were all equally expressed (Fig. S2*A*). β-Actin was included as the control for input loading, whereas eGFP was used as a measure for the transfection efficiency.

Insulin-Mediated Activation of TRPM6 Is Kinase Activity Independent. TRPM6 consists of an ion channel unit fused to an α-kinase. To determine whether the α-kinase domain plays a role in insulin-mediated stimulation of TRPM6 activity, HEK293T cells expressing the phosphotransferase-deficient mutant (17) TRPM6($K^{1804}R$) were treated for 1 h with 10 nM insulin. Whole-cell patch clamp analysis showed that insulin stimulated the activity of TRPM6 ($K^{1804}R$) channels similar to that of wild-type TRPM6 (Fig. 2 *C* and *D*). The I/V relations (Fig. 2*D*) and total protein expression (Fig. S2*B*) of the TRPM6 variants were comparable.

Cyclin-Dependent Kinase 5 Is Involved in TRPM6 Activation by Insulin. To deduce why the TRPM6 SNPs were insensitive to insulin, the molecular mechanism responsible for the insulin-induced TRPM6 stimulation was investigated. Cross-species protein sequence comparison showed potential phosphorylation sites in the proximity of the SNPs (Fig. 2 *E* and *F*). The NetPhosK server (http://www.cbs.dtu.dk/services/NetPhosK/) predicted T^{1391} as a potential phosphorylation target of cyclin-dependent kinase 5 (CDK5) and S^{1583} as a protein kinase A (PKA) or C (PKC) site. Roscovitine, an inhibitor of CDK5, abolished insulin-mediated

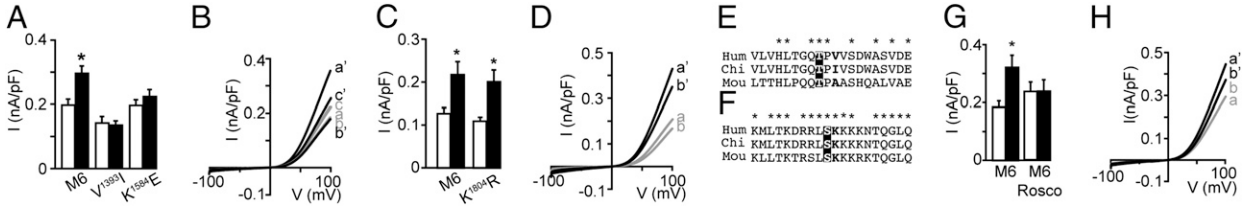

Fig. 2. Insulin does not stimulate the SNPs $V^{1393}I$ and $K^{1584}E$. (*A*) Average current density (nA/pF) of TRPM6, $V^{1393}I$, and $K^{1584}E$ channels expressing HEK293T cells with (■) and without (□) insulin pretreatment. (*B*) Average I/V relations of wild-type TRPM6, $V^{1393}I$, and $K^{1584}E$ without [*a* (n = 53), *b* (n = 30), *c* (n = 48)] or with [*a′* (n = 58), *b′* (n = 23), *c′* (n = 42)] 10 nM insulin pretreatment. (*C*) Average current density (nA/pF) of wild-type TRPM6 and TRPM6($K^{1804}R$) without (□) and with (■) insulin pretreatment. (*D*) I/V relationship of wild-type TRPM6 and TRPM6($K^{1804}R$), the phosphotransferase-deficient mutant, with [*a′* (n = 14), *b′* (n = 20)] and without [*a* (n = 13), *b* (n = 23)] insulin pretreatment respectively. (*E* and *F*) Cross-species protein sequence comparison highlighting the potential phosphorylation sites in the vicinity of the SNPs. (*G*) Average current density (nA/pF) of TRPM6-transfected HEK293T cells, pretreated with 20 μM roscovitine, the CDK5 inhibitor, with (■) or without (□) insulin pretreatment. (*H*) I/V relationship of TRPM6 with (*a′*, n = 19) or without insulin (*a*, n = 19) and TRPM6 and roscovitine (*b′*, n = 18) or without (*b*, n = 12) insulin pretreatment. Data in the histograms are shown as mean ± SEM *P < 0.05 compared with wild-type TRPM6.

stimulation of TRPM6 (Fig. 2*G*). Insulin (10 nM, 1 h) was added to the bath solution 20 min after starting the treatment with roscovitine (20 μM). The I/V relations of TRPM6 were not affected by roscovitine treatment (Fig. 2*H*). To substantiate the involvement of CDK5, the mRNA encoding the kinase was down-regulated by small-interference RNA. This treatment prevented the stimulatory action of insulin on TRPM6 channel activity and down-regulated CDK5 protein expression significantly (Fig. S2 *C* and *D*).

Phosphomimetic Substitution of T^{1391} and S^{1583} Recovers Insulin-Mediated Activation of TRPM6($V^{1393}I$) and TRPM6($K^{1584}E$). To confirm the role of T^{1391} in insulin-mediated TRPM6 activation, a phosphorylation-deficient mutant $T^{1391}A$ was constructed. Insulin (10 nM) treatment for 1 h did not affect the whole-cell current of this mutant (Fig. 3*A*). The I/V curves (Fig. 3*B*), basal activity, and protein expression (Fig. S3*A*) of TRPM6($T^{1391}A$) were identical to that of wild-type TRPM6. To pinpoint the exact role of T^{1391} in insulin-mediated TRPM6 activation, a channel mutant mimicking the phosphorylated state (TRPM6($T^{1391}D$)) was inserted in TRPM6($V^{1393}I$). Contrary to TRPM6($T^{1391}A$) and TRPM6($V^{1393}I$), 10 nM insulin treatment for 1 h increased both the TRPM6($T^{1391}D$) and the TRPM6($T^{1391}D$ + $V^{1393}I$)-mediated whole-cell current (Fig. 3 *C* and *D*). Protein expression of TRPM6($T^{1391}D$) and the TRPM6($T^{1391}D$ + $V^{1393}I$) was comparable to that of wild-type TRPM6 (Fig. S3*B*). To address the insensitivity of TRPM6($K^{1584}E$) activity to insulin, the phosphorylation-deficient mutant TRPM6($S^{1583}A$), the second site predicted by NetPhosK, the constitutive phosphorylation mimicking mutant TRPM6($S^{1583}D$) and the double mutant TRPM6($S^{1583}D$ + $K^{1584}E$) were constructed. Whole-cell patch clamp analysis after insulin (10 nM, 1 h) treatment of these mutants showed that S^{1583} is indeed necessary for insulin-mediated wild-type TRPM6 stimulation. Moreover, the insulin-dependent activation of TRPM6($K^{1584}E$) was recovered by the constitutive activity of S^{1583} (Fig. 3 *E–H*). The I/V relation and protein expression of the mutants were comparable to that of wild-type TRPM6 (Fig. 3 *F* and *H* and Fig. S3 *C* and *D*).

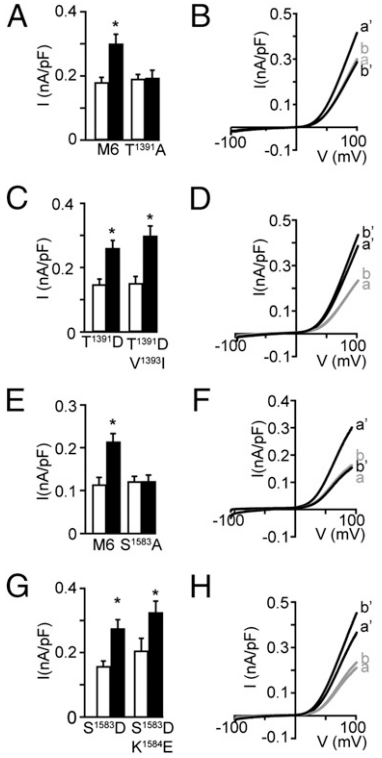

Fig. 3. Phosphorylation of T^{1391} and S^{1583} are necessary for insulin-mediated TRPM6 stimulation. (*A*) Average current density (nA/pF) of TRPM6 ($T^{1391}A$) and wild-type TRPM6 with (■) or without (□) insulin pretreatment. (*B*) I/V relationship of phosphorylation-deficient mutant TRPM6($T^{1391}A$) and wild-type TRPM6 with [*b′* (*n* = 26), *a′* (*n* = 25)] or without [*b* (*n* = 26), *a* (*n* = 23)] insulin pretreatment. (*C*) Average current density (nA/pF) of HEK293T cells expressing TRPM6($T^{1391}A$) and TRPM6($T^{1391}D$ + $V^{1393}I$) channels pretreated with (■) or without (□) insulin. (*D*) I/V relationship of the phosphorylation mimicking mutant TRPM6($T^{1391}D$) and TRPM6($T^{1391}D$ + $V^{1393}I$) with [*a′* (*n* = 16), *b′* (*n* = 12)] or without [*a* (*n* = 15), *b* (*n* = 11)] insulin pretreatment, respectively. (*E*) Histogram depicting the average current density (nA/pF) of TRPM6($S^{1583}A$) and wild-type TRPM6 with (■) or without (□) insulin pretreatment. (*F*) Corresponding I/V relationships [*a′* (*n* = 32), *b′* (*n* = 35), *a* (*n* = 28), *b* (*n* = 32)]. (*G*) Current density (nA/pF) of HEK293T cells expressing TRPM6($S^{1583}D$) and TRPM6($S^{1583}D$ + $K^{1584}E$) channels pretreated with (■) or without (□) insulin. (*H*) I/V relationships of TRPM6($S^{1583}D$) and TRPM6($S^{1583}D$ + $K^{1584}E$) with (*a′* (*n* = 25), *b′* (*n* = 23)] or without insulin [*a* (*n* = 21), *b* (*n* = 21)] pretreatment, respectively. Data in the histograms are shown as mean ± SEM **P* < 0.05 compared with wild-type TRPM6.

Activation of TRPM6 by Insulin Is PI3K and Rac1 Dependent. Phosphoinositide 3-kinases (PI3K) is one of the major downstream effectors of the IR signaling pathway (18, 19). To examine the involvement of PI3K in the insulin-mediated TRPM6 activation, two PI3K inhibitors (wortmannin and LY294002), were tested. Treatment with 20 nM wortmannin (added 20 min before insulin treatment) reduced the insulin-mediated stimulation of wild-type TRPM6 by 87 ± 6% (Fig. 4*A*), whereas basal activity of wild-type TRPM6 was not altered by wortmannin. A similar experiment with 10 μM LY294002 inhibited the insulin-mediated current by 66 ± 4% (Fig. 4*B*). LY294002 alone did not affect the basal activity of TRPM6. One of the common downstream effectors of PI3K, the Rho family GTPase Rac1, has been implicated in cytoskeleton rearrangement and protein trafficking (20–22). To address whether Rac1 is involved in TRPM6 activation by insulin, we used the constitutively active mutant Rac1($G^{12}V$) and dominant inactive mutant Rac1($T^{17}N$). HEK293T cells were cotransfected with wild-type TRPM6 and Rac1($G^{12}V$) or Rac1 ($T^{17}N$). As a control, HEK293T cells were cotransfected with TRPM6 and the empty vector. Cells coexpressing Rac1($T^{17}N$) and wild-type TRPM6 exhibited a comparable basal current to that of control cells. However, Rac1($T^{17}N$) prevented insulin-mediated increase in activity of wild-type TRPM6 (Fig. 4*C*). By contrast, TRPM6 cotransfection with Rac1($G^{12}V$) showed an increase in the wild-type TRPM6 basal activity. Furthermore, insulin treatment stimulated this basal activity (Fig. 4*C*).

Insulin Increases Cell Surface Expression of TRPM6. Increased TRPM6 activity by the Rac1($G^{12}V$) implies the notion that IR signaling promotes the mobility of TRPM6 containing endomembranes toward the plasma membrane. To this end, we used the potential of total internal reflection fluorescent (TIRF) microscopy to visualize the trafficking of eGFP–TRPM6-containing vesicles at the plasma membrane (22). Detailed observation of eGFP–TRPM6 in transiently transfected HEK293T cells using TIRF microscopy revealed a highly motile punctate distribution pattern. The fluorescence intensity of the cell in the TIRF plane was monitored and measured for 14 min before insulin application to obtain a basal intensity level (*Materials and Methods*) and subsequently for 22 min after application. The quantification of the fluorescence signals showed a clear augmentation of fluorescence intensity after insulin treatment (Fig. 4*D*). The first row of Fig. 4*E* shows the TIRF images of eGFP–TRPM6-expressing cells measured as a control at 0, 26, and 36 min. The second row of Fig. 4*E* depicts TIRF images before and 12 and 22 min after insulin application. The observed increase in fluorescence could be due to plasma membrane movement or expansion rather than trafficking of the vesicles. To address this

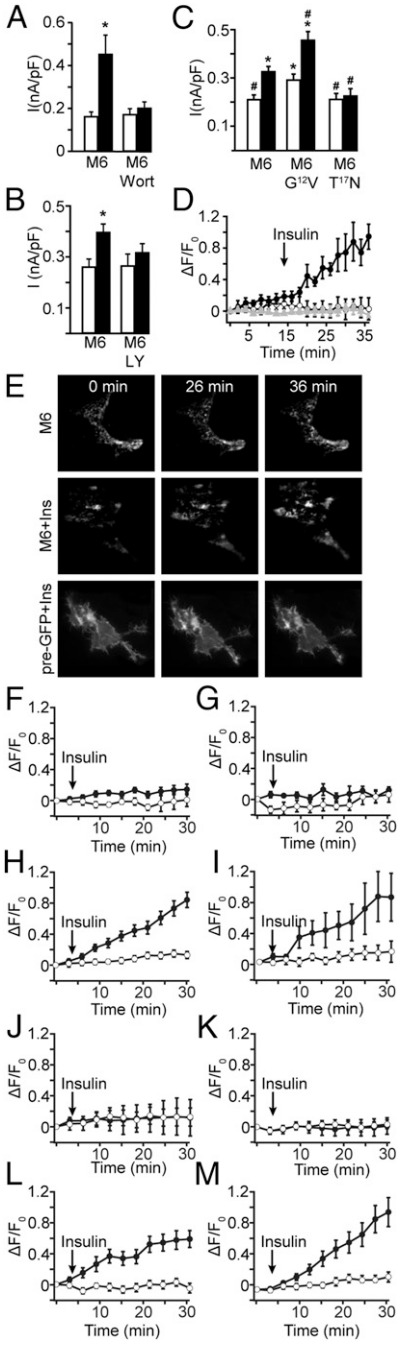

Fig. 4. Insulin increases the cell surface TRPM6 abundance in a PI3K- and Rac1-dependent manner. (*A*) Averaged current density of TRPM6-transfected HEK293T cells, pretreated with 20 nM wortmannin with (■) and without (□) insulin pretreatment. (*B*) Similar to panel *A*: untreated (□, n = 13), pretreated with 10 nM insulin (■, n = 13), pretreated with 10 μM LY294002 (□, n = 11) and pretreated with 10 μM LY294002 and insulin (■, n = 11). (*C*) Constitutively active mutant Rac1($G^{12}V$) stimulates wild-type TRPM6. Shown are the average current density (nA/pF) of wild-type TRPM6, TRPM6 cotransfected with Rac1($G^{12}V$), or Rac1($T^{17}N$) with (■, n = 43, 39, 19, from left to right, respectively) or without (□, n = 51, 36, 26, from left to right, respectively) insulin pretreatment. (*D*) Quantification of fluorescent intensity change over time in the control (○, n = 8) and insulin-treated conditions [●, eGFP–TRPM6 (n = 7), Δ, R-pre-GFP (n = 5)]. Arrow indicates addition of insulin to the bath in treatment conditions. (*E*) Representative TIRF images taken from the TRPM6 (○, control), TRPM6 insulin-treated (●), and insulin-treated R-pre-GFP (Δ) containing cells. (*F–M*) Insulin-mediated cell surface recruitment of TRPM6 is lost in TRPM6($V^{1393}I$) and TRPM6($K^{1584}E$) but is rescued by constitutive phosphorylation. (*F*) eGFP–TRPM6($V^{1393}I$), ○, n = 15; ●, n = 7. (*G*) eGFP–TRPM6($T^{1391}A$) ○, n = 5; ●, n = 3. (*H*) eGFP–TRPM6 ($T^{1391}D$) ○, n = 4; ●, n = 7. (*I*) eGFP–TRPM6($T^{1391}D$ + $V^{1393}I$) ○, n = 5; ●, n = 4. (*J*) eGFP–TRPM6($K^{1584}E$), ○, n = 5; ●, n = 6. (*K*) eGFP–TRPM6($S^{1583}A$) ○, n = 15; ●, n = 19. (*L*) eGFP–TRPM6($S^{1583}D$) ○, n = 11; ●, n = 7. (*M*) eGFP–TRPM6 ($S^{1583}D$ + $K^{1584}E$) ○, n = 10; ●, n = 16. Images are the average of 20 frames taken at 0.2-s intervals at the indicated time point. Data are shown as mean ± SEM $^{*}P < 0.05$ compared with wild-type TRPM6 and $^{\#}P < 0.05$ compared with wild-type TRPM6 pretreated with insulin.

point, HEK293T cells were transfected with R-pre-GFP (23), a plasma membrane marker, and subsequently insulin was applied. In Fig. 4*E*, the third row represents the images obtained before insulin application and 12 and 22 min after its application. Thus, the enhancement in fluorescent intensity of eGFP–TRPM6 upon insulin treatment is in line with an increase in the number of channels at the cell surface. These results were confirmed by cell surface biotinylation assays indicating that insulin increases cell surface expression of TRPM6. Importantly, total expression of TRPM6 was not affected by insulin (Fig. S4 *A* and *B*).

Rescue of Insulin-Mediated Cell Surface Recruitment of TRPM6($V^{1391}I$) and TRPM6($K^{1584}E$). Electrophysiological studies showed that T^{1391}, V^{1393}, S^{1583}, and K^{1584} residues are essential for insulin-dependent activation of TRPM6. To substantiate that the rescue of insulin-mediated activity of SNP baring channels was due to an increase in cell surface recruitment, appropriate phosphomimetic substitutions and SNPs were introduced into the eGFP–TRPM6 vector and subjected to TIRF analysis. Introducing the $V^{1391}I$ or $K^{1584}E$ mutation in TRPM6 or ablating of the proposed phosphorylation site $T^{1393}A$ or $S^{1583}A$ in close vicinity prevented insulin-mediated recruitment of TRPM6 to the cell surface (Fig. 4 *F*, *G*, *J*, and *K*). The cell surface recruitment of TRPM6($V^{1391}I$) was restored by introducing the phosphomimetic residue, $T^{1391}D$, into the channel. Similarly, introducing $S^{1583}D$ into TRPM6($K^{1584}E$) increased the cell surface accumulation upon insulin treatment (Fig. 4 *H*, *I*, *L*, and *M*). Coexpression of Rac1($G^{12}V$) did not restore cell surface recruitment in the absence of the appropriate phosphomimetic substitutions (Fig. S4 *C–I*).

Role of TRPM6 SNPs in Gestational Diabetes Mellitus. To assess the clinical relevance of our unique finding that, unlike TRPM6, TRPM6($V^{1393}I$) and TRPM6($K^{1584}E$) were not stimulated by insulin, 997 women from the Berlin Birth Cohort (BBC) (13, 14) were analyzed. Detailed data analysis of the entire study population including the maternal TRPM6($V^{1393}I$) and TRPM6 ($K^{1584}E$) genotypes is shown in Table 1 and Tables S1 and S2. Total glycosylated hemoglobin (TGH) level at delivery, as a measure of insulin resistance/glycemic control in this cohort of pregnant women who were nondiabetic and otherwise healthy before pregnancy, was measured. The more frequent SNP TRPM6($K^{1584}E$) was also associated with a higher likelihood of developing a significant impairment in glycemic control (TGH ≥ 7.0%). All carriers of the rare AA $V^{1393}I$ genotype were also carriers of the GG $K^{1584}E$ genotype. Therefore, the odds ratio for the more frequent GG $K^{1584}E$ genotype was calculated. The resulting odds ratio for TGH ≥ 7.0% for the maternal GG $K^{1584}E$ genotype was 4.59 (95% confidence interval: 1.59–13.23. (Table 1 and Tables S1 and S2). Here, we show that the two SNPs in TRPM6 are associated with altered TGH levels.

Discussion

The molecular etiology of hypomagnesemia and its clinical complications associated with insulin resistance and/or GDM/DM2 is poorly understood, despite a growing body of evidence

Table 1. Maternal TGH of the study population including maternal $V^{1393}I$ and $K^{1584}E$ genotypes

	Maternal $V^{1393}I$ genotype						
	Total	GG	GA	AA	Linear	*A rec*	*A dom*
N	986	790	189	7	*p*	*p*	*p*
Maternal TGH, %	6.3 ± 0.7	6.3 ± 0.7	6.2 ± 0.7	6.7 ± 0.9	0.09	0.04	0.81
Maternal TGH ≥ 7.0%	15.3	14.7	17.5	28.6	0.51	0.26	0.97
	Maternal $K^{1584}E$ genotype						
	Total	AA	AG	GG	Linear	*G rec*	*G dom*
N	997	677	294	26	*p*	*p*	*p*
Maternal TGH, %	6.3 ± 0.7	6.3 ± 0.7	6.2 ± 0.7	6.8 ± 0.8	0.001	<0.001	0.72
Maternal TGH ≥ 7.0%	15.8	15.5	14.6	38.5	0.002	0.01	0.13

Data are given as mean ± SEM or %. Odds ratios for TGH ≥ 7.0%: 4.59 (95% confidence intervals: 1.59–13.23) in maternal $K^{1584}E$ genotype G rec. Refer also to Tables S1 and S2.

depicting their relation. By using a combination of electrophysiological, biochemical, and live cell imaging techniques, we demonstrate that insulin stimulates the activity of TRPM6, but not that of TRPM6($V^{1393}I$) and TRPM6($K^{1584}E$). These SNPs have been predicted to be a risk factor for DM2 in elderly women under low Mg^{2+} intake (11). Moreover, we show that pregnant women carrying these SNPs, have higher TGH levels, indicating worsening of insulin resistance compared with those carrying wild-type TRPM6, signifying its role in the hypomagnesemia observed in GDM/DM2 patients.

Our data demonstrate that insulin increases the TRPM6 channel activity specifically by engaging the IR, whereas the channels harboring the SNPs lack insulin-dependent channel modulation. Of note, IR is expressed in the DCT, the site where TRPM6 facilitates transepithelial Mg^{2+} transport. Several experiments were conducted to explain the molecular mechanism behind the insensitivity of the TRPM6 variants to insulin. The role of the kinase activity present in TRPM6 was excluded by showing that the phosphotransferase-deficient mutant TRPM6($K^{1804}R$) was still stimulated by insulin (17). Cross-species sequence alignment of TRPM6 suggested the presence of two potential phosphorylation sites, TRPM6(T^{1391}) and TRPM6 (S^{1583}), in the vicinity of the SNPs. Ablation of one of these phosphorylation sites prevented insulin-mediated recruitment of TRPM6 to the cell surface, despite the presence of the other functional second phosphorylation site. In addition, mimicking constitutive phosphorylation at one of the phosphorylation sites ($T^{1391}D$ or $S^{1583}D$) did not result in a constitutively active TRPM6 because the other phosphorylation site also needs to be activated by insulin. From these results, we conclude that phosphorylation of both T^{1391} and S^{1583} is necessary for insulin-dependent activation of TRPM6, whereas phosphorylation of one of these residues is not sufficient.

The TRPM6 variants $V^{1393}I$ and $K^{1584}E$ are not sensitive to insulin. Importantly, this insulin-insensitivity of TRPM6($V^{1393}I$) and TRPM6($K^{1584}E$) could be rescued by inserting $T^{1391}D$ or $S^{1583}D$, into the respective genetic variants. Thus, our combined approach including TIRF microscopy and patch clamp analysis suggested that the identified SNPs interfere with insulin-mediated phosphorylation of TRPM6. However, we could not detect direct phosphorylation of TRPM6 by insulin. These findings suggest that phosphorylation of TRPM6 regions in proximity to the identified SNPs determines the insulin sensitivity of TRPM6.

The CDK5 inhibitor roscovitine abolished insulin-mediated TRPM6 activation, substantiating its functional role. It is possible that TRPM6($V^{1393}I$) decreases the phosphorylation probability by CDK5 at T^{1391}. Initially, CDK5 was implied in the regulation of neuronal functions including cytoskeletal remodeling and synaptic transmissions. Recently, an increasing array of evidence established its function and presence in non-neuronal cells as well (24). CDK5 has been shown as a regulator of the association between GLUT4 and the synaptotagmin homolog, E-syt1, to modulate glucose transport in adipocytes upon insulin stimulation (25).

PI3K is well established as one of the key enzymes, associated with the signaling downstream of the IR (19). For instance, the epidermal growth factor (EGF)-mediated activation of TRPM6 channels involves a PI3K-dependent process (22). Rho-GTPases are involved in cytoskeletal rearrangement, regulation of vesicular trafficking, and membrane processes (26). Here, we show that the inhibition of PI3K using wortmannin and LY294002 abrogate the insulin-mediated activation of TRPM6. Further, the dominant negative mutant of the Rho-GTPase, Rac1 [Rac1($T^{17}N$)], abolished insulin-dependent TRPM6 activation, whereas its constitutively active Rac1($G^{12}V$) mutant increased basal TRPM6 currents and augmented the channel activation by insulin significantly, compared with that of TRPM6 alone. In the absence of insulin, constitutively active Rac1($G^{12}V$) facilitates increased trafficking of TRPM6 to the plasma membrane. These data unequivocally show that Rac1 is a downstream mediator of the insulin-dependent TRPM6 activation. The involvement of PI3K and Rac1 in the TRPM6 activation suggests an altered endomembrane trafficking and their potential redistribution to the plasma membrane. A similar mechanism by insulin was described for the cationic channel TRPV2. In nonstimulated conditions, TRPV2 was mainly observed in the cytoplasm of MIN6 cells. Application of insulin induced translocation and insertion of TRPV2 in the plasma membrane, resulting in an increased calcium influx (27).

Given the fact that insulin activates the TRPM6 whole-cell current together with the increase in TIRF intensity it can be concluded that this hormone augments the number of functional channels at the cell surface (Fig. S5). In vivo, in the DCT, the number of TRPM6 channels on the plasma membrane is rate limiting and the physiological effect of insulin on channel activity will be even more significant. To date, endogenous TRPM6 channel activity has never been measured and is technically demanding due to the very low expression of the channel and the lack of a specific channel blocker.

In the present study, most importantly, we established clinical relevance of these noteworthy findings. Epidemiological research suggests that women who do have GDM bear an increased risk of DM2 in later life (1, 28). It is associated with a higher risk of maternal as well as offspring morbidity and mortality during pregnancy, at birth and later in life (1, 28). The major complications of this situation are preeclampsia, neonatal hypoglycemia, and respiratory distress syndrome (1, 28). Increased concentrations of pregnancy hormones like estrogen and progesterone

lead to lower fasting glucose concentrations and deposition of fat, delay in gastric emptying, and increased appetite. As gestation progresses, however, postprandial glucose concentrations steadily increase, indicating a diminished sensitivity to insulin. To maintain proper glucose control in pregnancy, maternal pancreatic β cells have to increase insulin secretion to counteract the corresponding fall in tissue sensitivity to insulin. Apparently, pregnant women who develop GDM are unable to increase their insulin production to compensate for the increased resistance to insulin (1, 28).

Postreceptor defects in the insulin-signaling cascade are implicated in the development of insulin resistance. Mg^{2+} is an essential cofactor for multiple enzymes involved in glucose metabolism including the IR function. Several cohort studies found an inverse association between Mg^{2+} intake and risk for diabetes or insulin resistance (29, 30). Pregnancy represents a unique situation of relative Mg^{2+} deficiency (31). We assume that this condition may synergistically increase the risk for impaired glucose tolerance beside the well-known effects of female sex hormones (1, 28). Our study clearly demonstrates that two genetic variants of the TRPM6 channel are associated with TGH levels. The more frequent genetic variant, TRPM6($K^{1584}E$), was associated with a higher likelihood of developing a significant impairment in glycemic control (Table 1).

To conclude, pregnant women carrying TRPM6($V^{1393}I$) and TRPM6($K^{1584}E$) possibly lack the physiological regulation of TRPM6 by insulin. Because Mg^{2+} is very important for β-cell function (5) and sensitivity of IRs to insulin (6, 12), we speculate that the presence of TRPM6($V^{1393}I$) and TRPM6($K^{1584}E$) in these women may lead to a hypomagnesemic state resulting in impaired β-cell function and insulin secretion and/or IR sensitivity. Therefore, these women develop an impaired glucose tolerance with a higher risk for GDM. These genetic variants of TRPM6 could be used as potential biomarkers to improve diagnosis and identify those at risk for developing GDM/DM2-induced hypomagnesemia. Importantly, similar to sodium-dependent glucose cotransporters (SGLT) (32, 33) the TRPM6 channel might serve as a renal target for drug development in the field of diabetes.

Materials and Methods

Subjects and Data Collection. A total of 997 women from the previously described Berlin Birth Cohort (BBC) (13, 14) were included in the study. Mean weight and mean blood pressure were calculated every trimester. At delivery, weights of the newborns were measured and maternal blood from a cubital vein was collected (See *SI Materials and Methods* for details).

TGH. Fetal and maternal blood was analyzed using the HPLCy-based variant TGH testing system (Bio-Rad) as described previously (14) (*SI Materials and Methods*).

Genotyping Using MALDI-TOF MS. Genomic fragments of the *TRPM6* gene containing the SNPs $V^{1393}I$ and $K^{1584}E$ were amplified in a multiplex PCR. For SNP detection, purified PCR products were mixed with the extension mix, polymorphism detection primers, and nucleotides to a final volume of 10 mL. The purified products were subjected to MALDI-TOF MS (*SI Materials and Methods*).

ACKNOWLEDGMENTS. We thank Dr. Kees Jalink and Dr. Elena Oancea for helpful discussions on total internal reflection fluorescence imaging. A.V.N., S.V., F.v.Z., R.J.B. and J.G.H. have been supported by Grant ZonMw 9120.8026 from the Netherlands Organization for Scientific Research and European Young Investigator Award C05.2134 from the European Science Foundation and the Dutch Kidney Foundation. M.K. was supported by the Peter-Stiftung für die Nierenwissenschaft (Nephrologie).

1. Reece EA, Leguizamón G, Wiznitzer A (2009) Gestational diabetes: The need for a common ground. *Lancet* 373:1789–1797.
2. Bellamy L, Casas JP, Hingorani AD, Williams D (2009) Type 2 diabetes mellitus after gestational diabetes: A systematic review and meta-analysis. *Lancet* 373:1773–1779.
3. Jovanovic-Peterson L, Peterson CM (1996) Vitamin and mineral deficiencies which may predispose to glucose intolerance of pregnancy. *J Am Coll Nutr* 15:14–20.
4. Bardicef M, et al. (1996) Perinatal cellular ion metabolism: 31P-nuclear magnetic resonance spectroscopic analysis of intracellular free magnesium and pH in maternal and cord blood erythrocytes. *J Soc Gynecol Investig* 3:66–70.
5. Barbagallo M, Dominguez LJ (2007) Magnesium metabolism in type 2 diabetes mellitus, metabolic syndrome and insulin resistance. *Arch Biochem Biophys* 458:40–47.
6. Barbagallo M, et al. (2003) Role of magnesium in insulin action, diabetes and cardiometabolic syndrome X. *Mol Aspects Med* 24:39–52.
7. Song Y, Manson JE, Buring JE, Liu S (2004) Dietary magnesium intake in relation to plasma insulin levels and risk of type 2 diabetes in women. *Diabetes Care* 27:59–65.
8. Volpe SL (2008) Magnesium, the metabolic syndrome, insulin resistance, and type 2 diabetes mellitus. *Crit Rev Food Sci Nutr* 48:293–300.
9. Wilson FH, et al. (2004) A cluster of metabolic defects caused by mutation in a mitochondrial tRNA. *Science* 306:1190–1194.
10. Meyer TE, et al.; Genetic Factors for Osteoporosis Consortium; Meta Analysis of Glucose and Insulin Related Traits Consortium (2010) Genome-wide association studies of serum magnesium, potassium, and sodium concentrations identify six Loci influencing serum magnesium levels. *PLoS Genet* 6:e1001045.
11. Song Y, et al. (2009) Common genetic variants of the ion channel transient receptor potential membrane melastatin 6 and 7 (TRPM6 and TRPM7), magnesium intake, and risk of type 2 diabetes in women. *BMC Med Genet* 10:4.
12. Paolisso G, Barbagallo M (1997) Hypertension, diabetes mellitus, and insulin resistance: The role of intracellular magnesium. *Am J Hypertens* 10:346–355.
13. Hocher B, et al. (2009) Fetal sex determines the impact of maternal PROGINS progesterone receptor polymorphism on maternal physiology during pregnancy. *Pharmacogenet Genomics* 19:710–718.
14. Pfab T, et al. (2006) Low birth weight, a risk factor for cardiovascular diseases in later life, is already associated with elevated fetal glycosylated hemoglobin at birth. *Circulation* 114:1687–1692.
15. Dai LJ, et al. (2001) Magnesium transport in the renal distal convoluted tubule. *Physiol Rev* 81:51–84.
16. Schäffer L, et al. (2008) A novel high-affinity peptide antagonist to the insulin receptor. *Biochem Biophys Res Commun* 376:380–383.
17. Cao G, et al. (2008) RACK1 inhibits TRPM6 activity via phosphorylation of the fused alpha-kinase domain. *Curr Biol* 18:168–176.
18. Kitamura T, Kahn CR, Accili D (2003) Insulin receptor knockout mice. *Annu Rev Physiol* 65:313–332.
19. Cantley LC (2002) The phosphoinositide 3-kinase pathway. *Science* 296:1655–1657.
20. Bezzerides VJ, Ramsey IS, Kotecha S, Greka A, Clapham DE (2004) Rapid vesicular translocation and insertion of TRP channels. *Nat Cell Biol* 6:709–720.
21. Sumita C, et al. (2005) Platelet activating factor induces cytoskeletal reorganization through Rho family pathway in THP-1 macrophages. *FEBS Lett* 579:4038–4042.
22. Thebault S, Alexander RT, Tiel Groenestege WM, Hoenderop JG, Bindels RJ (2009) EGF increases TRPM6 activity and surface expression. *J Am Soc Nephrol* 20:78–85.
23. Yeung T, et al. (2006) Receptor activation alters inner surface potential during phagocytosis. *Science* 313:347–351.
24. Rosales JL, Lee KY (2006) Extraneuronal roles of cyclin-dependent kinase 5. *Bioessays* 28:1023–1034.
25. Lalioti V, et al. (2009) The atypical kinase Cdk5 is activated by insulin, regulates the association between GLUT4 and E-Syt1, and modulates glucose transport in 3T3-L1 adipocytes. *Proc Natl Acad Sci USA* 106:4249–4253.
26. Symons M, Rusk N (2003) Control of vesicular trafficking by Rho GTPases. *Curr Biol* 13: R409–R418.
27. Hisanaga E, et al. (2009) Regulation of calcium-permeable TRPV2 channel by insulin in pancreatic beta-cells. *Diabetes* 58:174–184.
28. Kjos SL, Buchanan TA (1999) Gestational diabetes mellitus. *N Engl J Med* 341: 1749–1756.
29. Kirii K, Iso H, Date C, Fukui M, Tamakoshi A; JACC Study Group (2010) Magnesium intake and risk of self-reported type 2 diabetes among Japanese. *J Am Coll Nutr* 29: 99–106.
30. Villegas R, et al. (2009) Dietary calcium and magnesium intakes and the risk of type 2 diabetes: The Shanghai Women's Health Study. *Am J Clin Nutr* 89:1059–1067.
31. James MF (2010) Magnesium in obstetrics. *Best Pract Res Clin Obstet Gynaecol* 24: 327–337.
32. Kinne RK, Castaneda F (2011) SGLT inhibitors as new therapeutic tools in the treatment of diabetes. *Handb Exp Pharmacol* 1900:105–126.
33. Abdul-Ghani MA, Norton L, Defronzo RA (2011) Role of sodium-glucose cotransporter 2 (SGLT 2) inhibitors in the treatment of type 2 diabetes. *Endocr Rev* 32:515–531.